

## Original Article

# Methotrexate plus electroacupuncture reduces autophagy in ankle synovial tissue in rats with rheumatoid arthritis

Jianbin Sun<sup>1</sup>, Wendi Zhai<sup>2</sup>, Zheng Wang<sup>3</sup>, Weijun An<sup>4</sup>

<sup>1</sup>Department of Hand, Foot and Ankle, The General Hospital of Ningxia Medical University, Yinchuan 750004, Ningxia Hui Autonomous Region, P. R. China; <sup>2</sup>Department of Anesthesiology, Yinchuan Second People's Hospital, Yinchuan 750004, Ningxia Hui Autonomous Region, P. R. China; <sup>3</sup>Department of Orthopedics, The General Hospital of Ningxia Medical University, Yinchuan 750004, Ningxia Hui Autonomous Region, P. R. China; <sup>4</sup>Department of Trauma Orthopaedics, The General Hospital of Ningxia Medical University, Yinchuan 750004, Ningxia Hui Autonomous Region, P. R. China

Received December 7, 2022; Accepted March 13, 2023; Epub April 15, 2023; Published April 30, 2023

**Abstract:** Objective: To explore the effect of methotrexate combined with electroacupuncture on autophagy in the ankle synovial tissue in rats modeled with rheumatoid arthritis. Methods: A rat model of rheumatoid arthritis was constructed by Freund's complete adjuvant injection. The animals were then randomly grouped into the methotrexate + electroacupuncture, methotrexate, electroacupuncture, and model groups. The left hindfoot plantar volume, histopathological morphology of the ankle joint synovium, and autophagy-related genes were detected and compared after the intervention. Results: In comparison with the model group, significantly reduced plantar volume and mRNA and protein levels of autophagy-related gene (Atg) 3, Atg5, Atg12, unc-51-like kinase 1 (ULK1), Beclin1, and light chain 3 (LC3), as well as alleviated synovial hyperplasia were identified in the methotrexate and electroacupuncture groups. The improvement in the above indicators was more pronounced in the methotrexate + electroacupuncture group. Conclusions: By inhibiting autophagosome formation, both methotrexate and electroacupuncture inhibit synovial cell autophagy, alleviate synovial cell hyperautophagy, and relieve abnormal synovial hyperplasia, thus exerting a protective effect on the joint synovium. The combination of treatment with methotrexate and electroacupuncture works best.

**Keywords:** Methotrexate, electroacupuncture, rheumatoid arthritis rats, ankle synovial tissue, autophagy

## Introduction

Rheumatoid arthritis (RA) is a highly heterogeneous and chronic systemic autoimmune disease. The clinical manifestations of RA mostly start with the facet joints (mostly symmetrical) that affects the synovium of the joint and can erode articular cartilage and bone tissue as conditions worsen, resulting in structural destruction of the joint, loss of function, and deformities [1]. Pathologically, this manifests as inflammation and abnormal hyperplasia of the synovium, cartilage erosion, and bone destruction, which eventually leads to joint deformity and dysfunction, with a very high morbidity [2]. The hallmark pathological features of RA are abnormal proliferation of syno-

vial cells and synovial inflammatory response [3]. Studies have shown an association between autophagy and the pathological process of aberrant proliferation of synovial cells [4]. Continuous stimulation of the autophagy pathway can cause excessive activation and differentiation of synovial cells, and promote synovial cell proliferation, thus aggravating the condition of RA [5].

Methotrexate, a potent competitive inhibitor of dihydrofolate reductase, is the most widely used disease-modifying antirheumatic drug in the treatment of RA [6]. It has been reported that a weekly dose of 7.5-25 mg of methotrexate produces the best clinical outcomes in RA compared to the 5000 mg/week dose used to

treat malignancies [7]. In addition to its anti-inflammatory effects, methotrexate has also been shown to inhibit the proliferation of lymphocytes and macrophages [8]. Based on the relationship between the abnormal proliferation of cell membranes and autophagy, the effect of methotrexate on autophagy in RA is also worthy of attention. Besides medication, acupuncture has attracted more and more attention from clinicians due to its recognized efficacy in the treatment of RA [9]. It can protect vascular endothelial cells and synovial tissue by alleviating the inflammatory response of the affected limb, inhibiting the production of inflammatory mediators, thus fundamentally achieving the purpose of treating RA [10]. However, its mechanism remains unclear.

Currently, basic research on the use of methotrexate in combination with electroacupuncture in RA remains limited. The novelty of this study lies in the validation and analysis of the therapeutic feasibility and effectiveness of methotrexate combined with electroacupuncture in RA rat model from the perspectives of left hind-foot plantar volume, microstructural changes of synovial cells in RA model rats, and mRNA and protein expression of autophagy-related genes. This paper gives novel insights into the mechanism of action of the combination therapy in RA treatment and provides new clinical evidence for the selection of treatment regimens for RA, with great clinical implications for improving the condition of RA and exploring new therapeutic mechanisms of RA.

### Materials and methods

#### *Establishment of a rat RA model*

Fifty Specific pathogen Free (SPF)\_male healthy Sprague Dawley (SD) rats (Changzhou Cavens Laboratory Animal Co., Ltd.) with a body weight of (180±20) g were reared under a temperature of 25-27°C, a humidity of 50-60%, and an alternating 12 h light-12 h dark cycle, with food and water provided adequately. The animals were grouped into a model group (n=40) and a control group (n=10) after 1 week of adaptive feeding. Rats in the model group were injected with the Freund's complete adjuvant (FCA; Shanghai Yuduo Biotechnology Co., Ltd., YLY1217) to build a RA rat model [11]; rats were anesthetized with isoflurane (Shanghai Jinsui Biotechnology Co., Ltd., J66928) and

immobilized. Then, 0.1 mL of FCA was injected subcutaneously under the left foot pad toward the ankle joint. The control group was injected with the same amount of 0.9% sodium chloride solution (Beijing Zeping Technology Co., Ltd., J/7590C/05). Successful modeling was indicated by the presence of acute inflammatory swelling from the left toe to the ankle 24 h after modeling, as well as persistent swelling and color change of the left ankle about 3 days after modeling, and redness and swelling or inflammatory nodules in the contralateral limb or forelimb, ear and tail. Animal experiments have been approved by the Animal Ethics Committee of the General Hospital of Ningxia Medical University.

#### *Intervention methods*

Model group rats were further randomly assigned to model, methotrexate, electroacupuncture, and methotrexate + electroacupuncture groups, with 10 rats in each group. The model group was not given any treatment. One day after successful modeling, rats in the methotrexate group were given 0.75 mg/kg methotrexate tablets (Beijing Pufei Biotechnology Co., Ltd., PB3737), which was made into powder and administered by gavage, after dissolving the drug in 1.5 mL of drinking water, 1 time/d for 6 days. In the electroacupuncture group, rats were first immobilized with a special rat immobilizer. Then, a 0.25 mm × 13 mm acupuncture needle was inserted straight into the Zusanli acupoint (ST36) at a depth of 3-4 mm. The left and right Zusanli acupoints were alternately electro-acupunctured every other day, with the dilatational wave frequency set as 20 Hz/50 Hz, the intensity deemed appropriate was for slight jitter of the needle handle, and the needle retained in place for 20 min. The rats received electroacupuncture 6 days a week with one day off. The animals in the methotrexate + electroacupuncture group were given methotrexate and electroacupuncture 1 day after modeling, with the same methods as described in the methotrexate group and the electroacupuncture group.

#### *Evaluation and comparison of joint swelling of rats in each group*

In this experiment, the plantar volume of rats was used to evaluate the degree of joint swelling. The next day after the last intervention, the

**Table 1.** Primer expression of each gene

Gene	Upstream	Downstream
Atg5	5'-TCCAACGTGCTTTACTCTCTATC-3'	5'-TGTCAGTTACCAGCGTCAAATA-3'
Atg12	5'-GCCTCGGAGCAGTTGTTTA-3'	5'-ATGTAGGACCAG-TTTACCATCAC-3'
Atg3	5'-GTGGCAGCTGGAGATCACTT-3'	5'-ACACCGCTTGATGCATGGAA-3'
β-actin	5'-CCCATCTATGAGGGTTACGC-3'	5'-TTTAATGTCACGCACG-ATTTC-3'

Note: Atg, autophagy-related gene.

left hind paw plantar volume of rats in each group was measured using a plantar volume meter following its instructions. Briefly, a mark was made on the ankle joint of the rat with a marker. The rat was then held at the left rear knee joint, the hind foot was straightened and slowly placed into a measuring cup. When the horizontal surface of the measuring cup overlapped with the measuring line of the rat's foot, the measuring switch was activated and the measuring data were recorded. The volume of toes on the 3rd, 9th, 15th, and 21st days after modeling was selected for statistical analysis.

*Observation of histopathological morphology of rat ankle joint synovium by hematoxylin-eosin (H&E) staining*

The rat hind limb 2 cm above the left ankle joint was quickly cut off by orthopedic scissors, and the hair and the surrounding excess soft tissue were removed. After 1-2 washes with Phosphate Buffered Saline (PBS; Beijing Kaishiyuan Biotechnology Co., Ltd., SH-0788) solution, the entire joint cavity was exposed with a blade incision, and the synovial tissue (the pale yellow smooth and translucent tissue attached under the ankle joint cartilage, about 0.2 cm × 0.1 cm in size) was cut with ophthalmic scissors. The samples were then blotted dry using filter paper, with one portion frozen in liquid nitrogen for H&E staining and Western blot detection, and the other for examination under transmission electron microscopy. Partial frozen synovial tissue was fastened in 4% paraformaldehyde, decalcified in Ethylene Diamine Tetraacetic Acid (EDTA; Beijing Solarbio Technology Co., Ltd., C1034) solution (10%), embedded in conventional paraffin, and sectioned by a microtome (thickness 4-5 μm), followed by xylene (Beijing Zeping Technology Co., Ltd., C42268.AP) deparaffinization, and anhydrous Ethanol (Shanghai LMAI Bio Co. Ltd., LM64-17-5) dehydration. After 30 min of staining with hematoxylin solution (Beijing Fubo

Biotechnology Co., Ltd., ab220365), the slices were rinsed with tap water and separated with 1% hydrochloric acid and ethanol. Following another rinse with tap water and counterstaining with 0.5%-0.1% eosin solution (Jiangxi IBIO Biotechnology Co., Ltd., IBIO-C780), the slices were dehydrated with gradient ethanol, cleared with xylene, and mounted with neutral gum. Morphological changes of the ankle joint synovial membrane were observed under a 200-fold light microscope and photographed using the Bx-70 Micro-Imaging System.

*Comparison of the levels of autophagy-related genes*

The messenger RNA (mRNA) levels of autophagy-related genes (Atgs) in synovial tissue were detected using fluorescence quantitative Polymerase Chain Reaction (PCR). The specific operation took 100 mg of left hindlimb plantar synovial tissue from the rat, which was cut into pieces and ground with liquid nitrogen. RNA was then extracted following kit (Beijing GenStar Biotechnology Co., Ltd., P118) instructions for reverse transcription. One μL of reverse-transcribed complementary DNA (cDNA) was utilized as the template for fluorescence quantitative PCR, and the reaction system consisted of 2 × SYBR Green mixture (5 μL; Beijing Solarbio Technology Co., Ltd., SY1020), downstream and upstream primers (each with 1 μL), and RNase-free water (2 μL). Reaction conditions were as follows: predenaturation at 95°C for 1 min; denaturation at 95°C for 5 s, and annealing/extension at 61°C for 10 s, for 40 cycles (Table 1).

*Western blot*

One hundred mg of rat left hindlimb plantar synovial tissue was taken and lysed by Radio Immuno Precipitation Assay (RIPA; Beijing Solarbio Technology Co., Ltd., R0020-100), and the protein concentration was measured using

## Electroacupuncture and rheumatoid arthritis

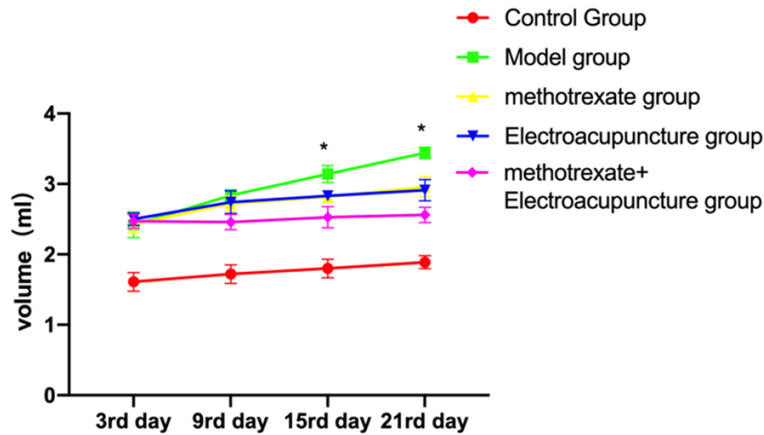


**Figure 1.** Comparison of left plantar volume of rats in each group. Note: \*means  $P < 0.05$  vs. control group.

a bicinchoninic acid (BCA) protein quantification kit (Shanghai Acme Biochemical Co., Ltd., PC0020-500). After isolation with 10% sodium dodecyl sulfate (SDS)-polyacrylamide gel (Shanghai Life iLab Biotech Co., Ltd., AP15L534), they were transferred to a polyvinylidene fluoride (PVDF) membrane (Beijing Yita Biotechnology Co., Ltd., YC0430), sealed with 5% nonfat dry milk (Shanghai Lianshuo Baowei Biotechnology Co., Ltd., AS0119) at room temperature for 2 hours and cultured at 4°C overnight with the following primary antibodies: light chain-3B (LC3B; 1:1000), unc-51-like kinase 1 (ULK1; 1:1000), Beclin-1 (1:2000), and glyceraldehyde-3-phosphate dehydrogenase (GAPDH; 1:1000). Subsequently, horseradish peroxidase (HRP)-conjugated anti-rabbit immunoglobulin G (IgG; Quanzhou Leda Qibo Biotechnology Co., Ltd., LDQB-A1-10025; 1:2000) was placed into the membrane and cultured under room temperature for 2 hours. After 3 rinses with TBST buffer (Wuhan Abclonal Biotech Co., Ltd., RM00013\_5L), the binding of secondary antibodies was identified using an enhanced chemiluminescence (ECL) system (Pierce Biotechnology, Rockford, USA). GAPDH was used as the internal control.

### Statistical methods

SPSS19.0 was used for statistical analysis and GraphPad 7 for image rendering and export. The measurement data were represented by mean  $\pm$  standard error of the mean (SEM), and the Student's *t* test, one-way analysis of variance, and LSD-*t* test were used for inter-group, multi-group, and post-hoc comparisons, res-

pectively.  $P < 0.05$  was taken as the significance level.

### Results

#### Comparison of left toe volume

Model group rats had a markedly higher left hindfoot plantar volume than control rats ( $P < 0.01$ ); compared with the model group, rats in methotrexate, electroacupuncture, and methotrexate + electroacupuncture groups all showed a marked reduction in the left hindfoot plantar volume from the 15th day after treatment ( $P < 0.01$ ), with the most significant reduction found in methotrexate + electroacupuncture treated rats ( $P < 0.05$ , **Figure 1**).

#### Comparison of histopathological morphology of rat ankle synovial tissue in each group

In the control group, the rat synovial tissue was smooth and transparent without hyperemia or hypertrophy, and the synovial cells were clear without swelling and deformation, nor obvious inflammatory cell infiltration; as for the model group, obvious hyperplasia of the synovial lining and disordered arrangement of synovial cells were observed, with increased edema in some cells, fibrous tissue hyperplasia, and inflammatory cell infiltration; the synovial morphology was partially thickened in both methotrexate and electroacupuncture groups, and the inflammatory cell infiltration was reduced compared with the model group; and in the methotrexate + electroacupuncture group, the synovial morphology was evidently improved compared with the model group, with alleviated synovial hyperplasia and reduced infiltration of inflammatory cells. In addition, the histopathological score was the lowest in the control group among the five groups; compared with the model group, the scores of methotrexate, electroacupuncture, and methotrexate + electroacupuncture groups were significantly lower; and a lower histopathological score was observed in the methotrexate + electroacupuncture group compared to methotrexate and electroacupuncture groups, as shown in **Figure 2**.

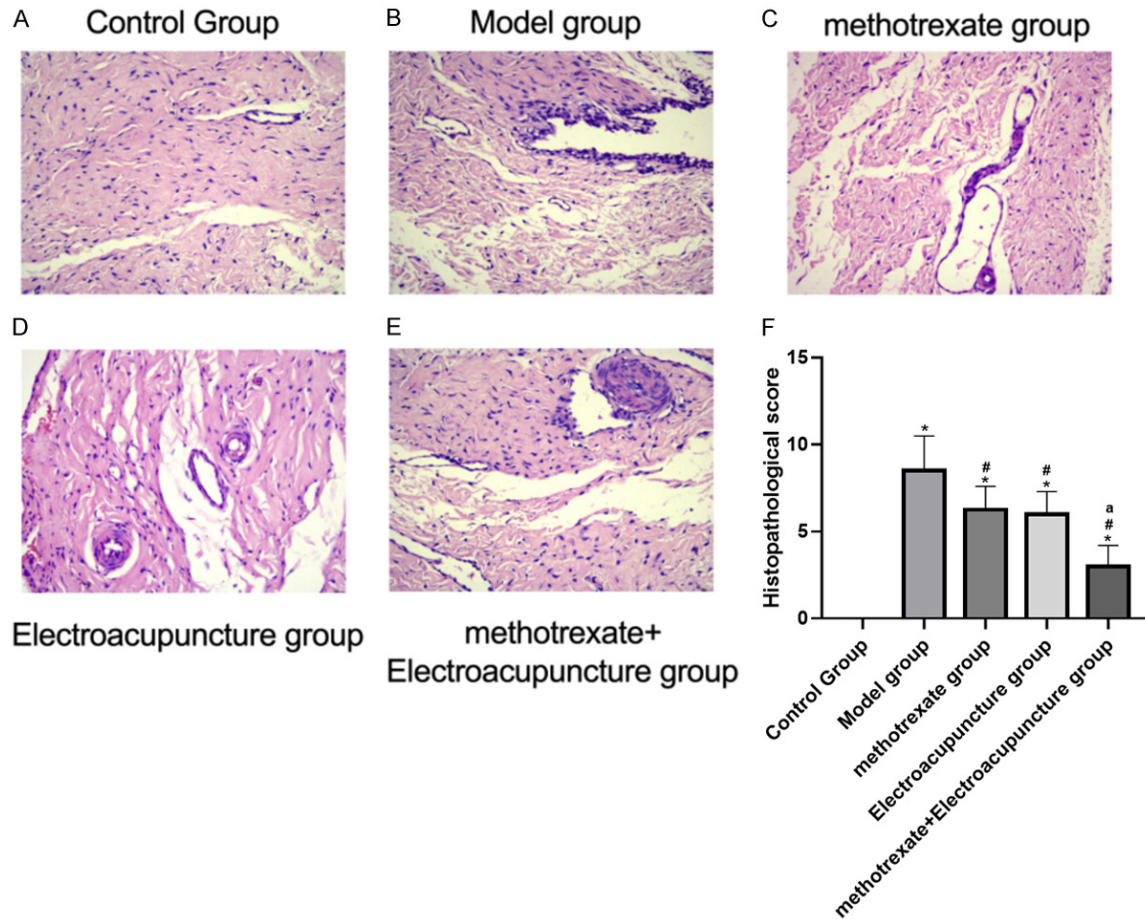


**Figure 2.** Comparison of the pathological morphology of the synovial membrane of the ankle joint of rats (H&E staining); A-E: Histopathological morphology of rat ankle joint synoviums; F: Histopathological scores of the five groups of rats. H&E, hematoxylin-eosin staining.

*Comparison of Atg3, Atg5, Atg12 mRNA and protein expression*

The model group showed evidently up-regulated mRNA and protein levels of Atg3, Atg5 and Atg12 in the synovial tissue than control rats ( $P < 0.01$ ); while all these indexes decreased markedly in methotrexate, electroacupuncture, and methotrexate + electroacupuncture groups compared to model group ( $P < 0.01$ ), with the highest reduction identified in the methotrexate + electroacupuncture group ( $P < 0.01$ ) **Figure 3**.

*Comparison of ULK1, Beclin1 and LC3-II mRNA and protein levels*

Evidently up-regulated mRNA and protein levels of ULK1, Beclin1 and LC3-II were determined in model group rats as compared to control rats ( $P < 0.01$ ,  $P < 0.05$ ); marked reductions in these

indexes were found in methotrexate, electroacupuncture, and methotrexate + electroacupuncture groups versus the model group ( $P < 0.05$ ,  $P < 0.01$ ), with their lowest levels found in the methotrexate + electroacupuncture group ( $P < 0.01$ ) **Figure 4**.

**Discussion**

As a systemic autoimmune disease, RA manifests itself primarily through chronic inflammation of joint tissue. Given the slow course of the disease and the fact that most patients are hardly aware of the disease at the initial stage, there is an urgent need to clarify the pathogenesis of RA and explore efficient treatment methods [12].

In this study, it was found that the rat plantar volume was significantly increased, and the histopathological morphology of the ankle synovi-

## Electroacupuncture and rheumatoid arthritis

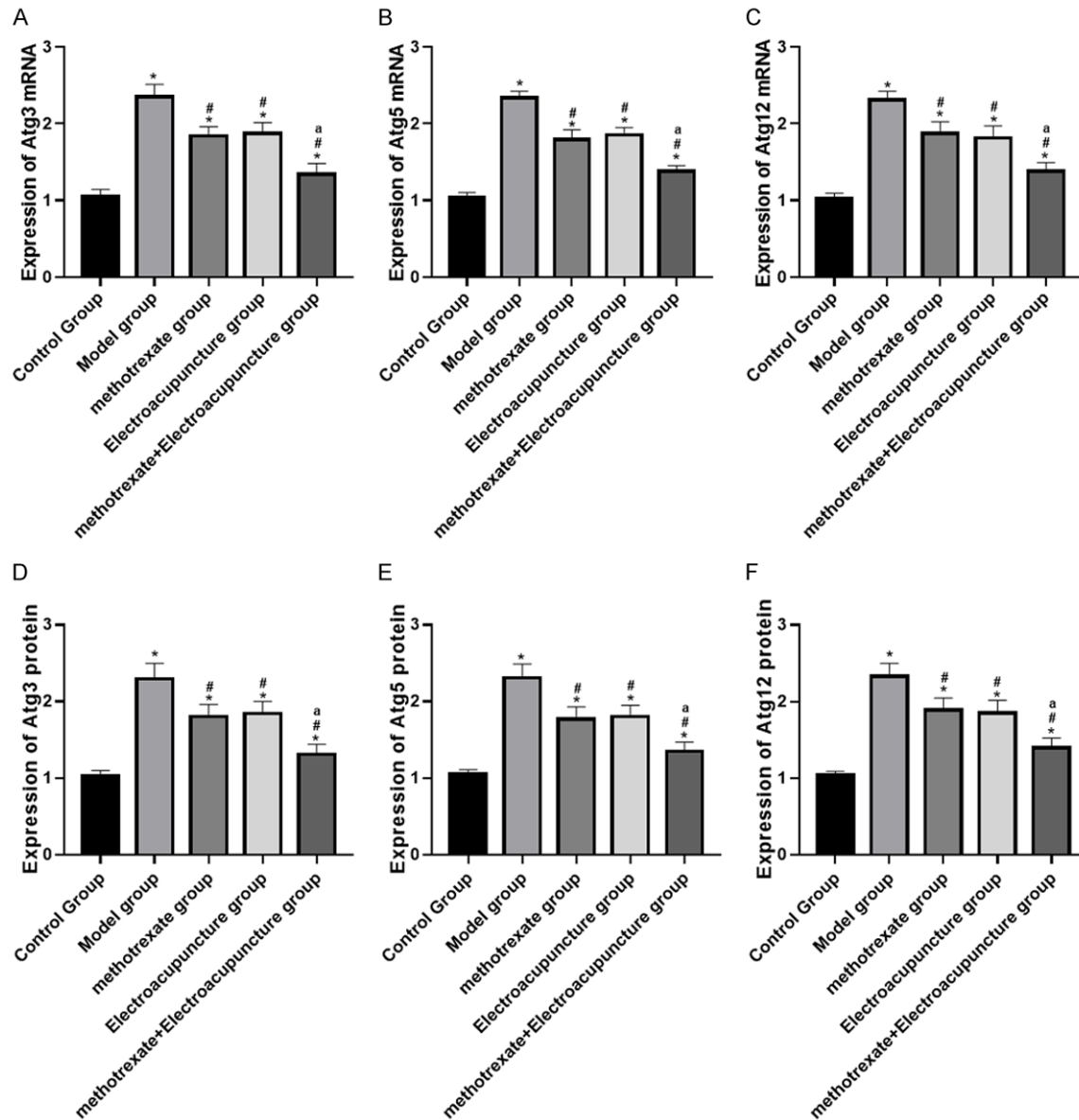


**Figure 3.** Comparison of Atg3, Atg5 and Atg12 mRNA and protein levels in synovial tissue of rats; A: Comparison of Atg3 mRNA levels among five groups of rats; B: Comparison of Atg5 mRNA levels among five groups of rats; C: Comparison of Atg12 mRNA levels among five groups of rats; D: Comparison of Atg3 protein levels among five groups of rats; E: Comparison of Atg5 protein levels among five groups of rats; F: Comparison of Atg12 protein levels among five groups of rats. \*indicates  $P < 0.05$ . Atg, autophagy; mRNA, messenger RNA.

al membrane was obvious in the model group; while both the plantar volume and pathological morphology were significantly alleviated under the intervention of methotrexate and electroacupuncture, and this improvement effect was more significant in the methotrexate + electroacupuncture group. This suggested that methotrexate + electroacupuncture can more effectively reduce toe swelling and pathological progression in RA rats, with significant effects

in relieving pathological symptoms and morphological manifestations. Methotrexate, as one of the earliest cancer chemotherapy drugs, has been recently revealed to be able to regulate T lymphocytes and improve the immune function of the body, thereby inhibiting RA progression [13, 14]. In addition, the mechanism by which electroacupuncture stimulates “Zusanli” to improve the abnormal proliferation of synovial cells in RA may be related to its inhi-

## Electroacupuncture and rheumatoid arthritis

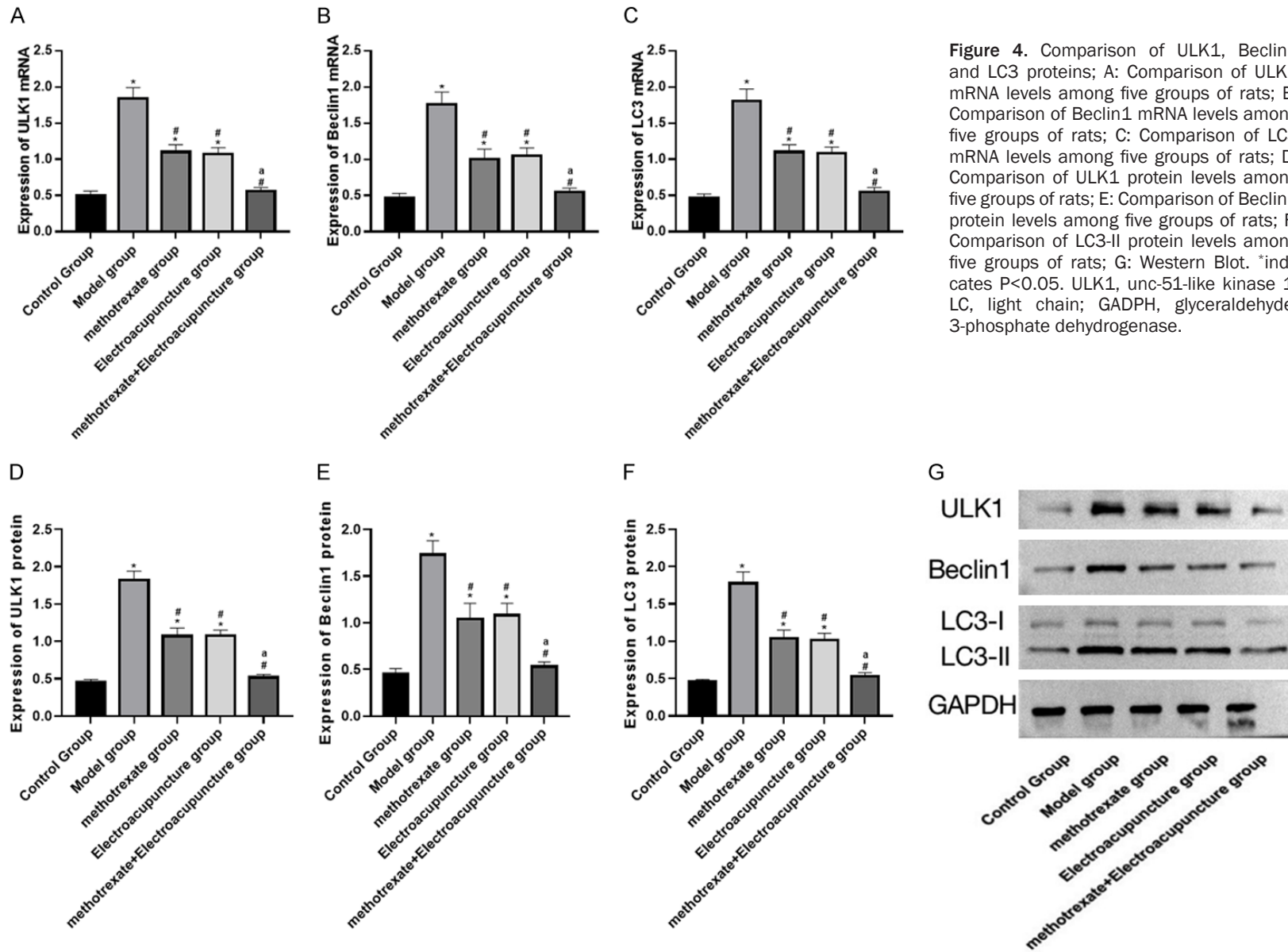


**Figure 4.** Comparison of ULK1, Beclin1 and LC3 proteins; A: Comparison of ULK1 mRNA levels among five groups of rats; B: Comparison of Beclin1 mRNA levels among five groups of rats; C: Comparison of LC3 mRNA levels among five groups of rats; D: Comparison of ULK1 protein levels among five groups of rats; E: Comparison of Beclin1 protein levels among five groups of rats; F: Comparison of LC3-II protein levels among five groups of rats; G: Western Blot. \*indicates  $P < 0.05$ . ULK1, unc-51-like kinase 1; LC, light chain; GAPDH, glyceraldehyde-3-phosphate dehydrogenase.

bition of synovial cell autophagy [15]. Another study indicated that the inhibition of electroacupuncture against RA in rats was related to the regulation of nuclear factor  $\kappa$ B (NF- $\kappa$ B) pathway and tumor necrosis factor  $\alpha$  (TNF- $\alpha$ ) [16]. All of the above helps explain the effective and prominent improvement of RA under the combined intervention of methotrexate and electroacupuncture. Meanwhile, Zhou Y et al. [17] reported that methotrexate + electroacupuncture in RA patients with liver and kidney deficiency can significantly reduce their clinical symptoms, similar to our findings. Liu L et al. [18] also pointed out that the palliative effect of methotrexate + electroacupuncture on synovitis in RA rats was related to the promotion of synovial cell apoptosis and the activation of Factor-related Apoptosis (Fas)/Fas Ligand (FasL) axis. The preceding research may help explain the anti-RA treatment mechanism of methotrexate + electroacupuncture.

To further understand the anti-RA mechanism of this combination therapy, we analyzed the effects of methotrexate and electroacupuncture on autophagy. Autophagy is a process in which intracellular lysosomes catabolize their own organelles and cytoplasm, which plays a vital role in RA occurrence and progression. The autophagy process is mainly regulated by a series of complexes formed by Atgs, and these proteins are crucial in the initiation of autophagy and the formation, extension, maturation, and degradation of autophagic vacuoles [19]. Atg3, Atg5, Atg12, ULK1, Beclin1, and LC3 are all autophagy related indicators; their mRNA and protein levels can be used to evaluate the process of RA-related autophagy, with their up-regulated levels closely associated with disease deterioration of RA [20, 21]. In our research, all the above autophagy-related indexes presented markedly elevated mRNA and protein levels in model group rats than in control rats, while they were significantly inhibited in methotrexate, electroacupuncture, and methotrexate + electroacupuncture groups, with even lower levels in methotrexate + electroacupuncture group. This indicates that the autophagy process can be controlled to alleviate the pathological progression of RA under methotrexate + electroacupuncture treatment, which was consistent with the results of Liu L et al. [22]. According to Xu K et al. [23], the regulation of autophagy by methotrexate is related

to its mediation of autophagosome formation and participation in the regulation of high-mobility group box protein 1 (HMGB1) and Beclin1 expression. There have also been many reports on the regulatory mechanism of electroacupuncture in the process of autophagy. Pan XL et al. [24], for example, pointed out that the electroacupuncture at Zusanli acupoint can alleviate excessive autophagy of interstitial cells of Cajal by inhibiting the AMP-activated kinase (AMPK)/ULK1 pathway, thereby improving functional dyspepsia in rats. As reported by Wang MM et al. [25], the autophagy regulation mechanism exerted by electroacupuncture in ischemic stroke is related to its activation of the phosphatidylinositol-3-kinase (PI3K)/protein kinase B (AKT) pathway. All of the above reports help to explain the underlying mechanism of action of electroacupuncture in RA treatment.

The limitations of this study are as follows: first, the molecular pathways that regulate or affect autophagy have not been explored to dig deeper into the underlying mechanisms; second, synovial cell proliferation and synovial inflammatory response should be analyzed to verify the effects of methotrexate combined with electroacupuncture on disease progression in RA model rats; third, the effect of time on the anti-RA effect of methotrexate combined with electroacupuncture was not considered. In the future, supplementary analyses will be carried out to address the above deficiencies, so as to further improve this research project.

In summary, this study suggests that both methotrexate and electroacupuncture may inhibit the autophagy activity of synovial cells by inhibiting autophagosome formation, relieve excessive autophagy in synovial cells, and alleviate the abnormal proliferation of the synovium, to achieve the purpose of protecting the joint synovium, with better efficacy when used in combination. Whether it can inhibit synovial cell proliferation through other pathways needs further study.

### Disclosure of conflict of interest

None.

**Address correspondence to:** Jianbin Sun, Department of Hand, Foot and Ankle, The General

## Electroacupuncture and rheumatoid arthritis

Hospital of Ningxia Medical University, Yinchuan 750004, Ningxia Hui Autonomous Region, P. R. China. Tel: +86-13469607040; E-mail: 13469607040@163.com

### References

- [1] Szostak B, Machaj F, Rosik J and Pawlik A. Using pharmacogenetics to predict methotrexate response in rheumatoid arthritis patients. *Expert Opin Drug Metab Toxicol* 2020; 16: 617-626.
- [2] Rheumatoid arthritis. *Nat Rev Dis Primers* 2018; 4: 18002.
- [3] Feng FB and Qiu HY. Effects of Artesunate on chondrocyte proliferation, apoptosis and autophagy through the PI3K/AKT/mTOR signaling pathway in rat models with rheumatoid arthritis. *Biomed Pharmacother* 2018; 102: 1209-1220.
- [4] Chadha S, Behl T, Bungau S, Kumar A, Kaur R, Venkatachalam T, Gupta A, Kandhwal M and Chandel D. Focus on the multimodal role of autophagy in rheumatoid arthritis. *Inflammation* 2021; 44: 1-12.
- [5] Zhao J, Jiang P, Guo S, Schrodi SJ and He D. Apoptosis, autophagy, netosis, necroptosis, and pyroptosis mediated programmed cell death as targets for innovative therapy in rheumatoid arthritis. *Front Immunol* 2021; 12: 809806.
- [6] Cronstein BN and Aune TM. Methotrexate and its mechanisms of action in inflammatory arthritis. *Nat Rev Rheumatol* 2020; 16: 145-154.
- [7] Bluett J, Riba-Garcia I, Verstappen SMM, Wendling T, Ogunbenro K, Unwin RD and Barton A. Development and validation of a methotrexate adherence assay. *Ann Rheum Dis* 2019; 78: 1192-1197.
- [8] Yan H, Su R, Xue H, Gao C, Li X and Wang C. Pharmacomicrobiology of methotrexate in rheumatoid arthritis: gut microbiome as predictor of therapeutic response. *Front Immunol* 2021; 12: 789334.
- [9] Li HX, Zhao W, Shi Y, Li YN, Zhang LS, Zhang HQ and Wang D. Retinoic acid amide inhibits JAK/STAT pathway in lung cancer which leads to apoptosis. *Tumour Biol* 2015; 36: 8671-8678.
- [10] Malemud CJ. The role of the JAK/STAT signal pathway in rheumatoid arthritis. *Ther Adv Musculoskelet Dis* 2018; 10: 117-127.
- [11] Steinmetz M, Laurans L, Nordsiek S, Weiss L, van der Veken B, Ponnuswamy P, Esposito B, Vandestienne M, Giraud A, Gobbel C, Steffen E, Radecke T, Potteaux S, Nickenig G, Rassaf T, Tedgui A and Mallat Z. Thymic stromal lymphopoietin is a key cytokine for the immunomodulation of atherogenesis with Freund's adjuvant. *J Cell Mol Med* 2020; 24: 5731-5739.
- [12] Tekaya R, Triki W, Ben Tekayen A, Saidane O, Mahmoud I and Abdelmoula L. Is compliance to methotrexate in rheumatoid arthritis different in Tunisian patients? *Therapie* 2021; 76: 260-263.
- [13] Rajitha P, Biswas R, Sabitha M and Jayakumar R. Methotrexate in the treatment of psoriasis and rheumatoid arthritis: mechanistic insights, current issues and novel delivery approaches. *Curr Pharm Des* 2017; 23: 3550-3566.
- [14] Yazici Y and Bata Y. Parenteral methotrexate for the treatment of rheumatoid arthritis. *Bull Hosp Jt Dis (2013)* 2013; 71 Suppl 1: 46-48.
- [15] Luo H, Peng J, Ma Q, Wei Z, Lin C, Zhang M, Li P, Song Y and Yang X. Intradermal acupuncture for rheumatoid arthritis: study protocol for a randomised controlled trial. *Trials* 2021; 22: 450.
- [16] Li J, Li J, Chen R and Cai G. Targeting NF-kappaBeta and TNF-alpha activation by electroacupuncture to suppress collagen-induced rheumatoid arthritis in model rats. *Altern Ther Health Med* 2015; 21: 26-34.
- [17] Zhou Y, Zhu J, Li LB, He TF, Chen XY, Zheng YY and Chen YF. Effects of Electroacupuncture on Joint Function in rheumatoid arthritis patients of liver- and kidney-yin deficiency type. *Zhen Ci Yan Jiu* 2016; 41: 440-446.
- [18] Liu L, Zhou W, Li MY, Zhou L, Zhang L, Wang WY, Gong ZX and Ai K. Effect of electroacupuncture of "Zusanli" (ST36) and "Guanyuan" (CV4) on apoptosis and expression of apoptosis-related proteins of synoviocytes in adjuvant-induced arthritis rats. *Zhen Ci Yan Jiu* 2022; 47: 696-702.
- [19] Iftikhar R, Chaudhry QUN, Anwer F, Neupane K, Rafae A, Mahmood SK, Ghafoor T, Shahbaz N, Khan MA, Khattak TA, Shamsad GU, Rehman J, Farhan M, Khan M, Ansar I, Ashraf R, Marsh J, Satti TM and Ahmed P. Allogeneic hematopoietic stem cell transplantation in aplastic anemia: current indications and transplant strategies. *Blood Rev* 2021; 47: 100772.
- [20] Hao F, Wang Q, Liu L, Wu LB, Cai RL, Sang JJ, Hu J, Wang J, Yu Q, He L, Shen YC, Miao YM, Hu L and Wu ZJ. Effect of moxibustion on autophagy and the inflammatory response of synovial cells in rheumatoid arthritis model rat. *J Tradit Chin Med* 2022; 42: 73-82.
- [21] Xu L and Pan J. Transcription factor EB promotes rheumatoid arthritis of Sprague-Dawley rats via regulating autophagy. *3 Biotech* 2021; 11: 162.
- [22] Liu L, Zhou W, Li MY, Zhou L, Wang WY, Gong ZX and Ai K. Effect of electroacupuncture on autophagy in synovial tissues of rheumatoid

## Electroacupuncture and rheumatoid arthritis

- arthritis rats. *Zhen Ci Yan Jiu* 2021; 46: 1023-1028.
- [23] Xu K, Cai YS, Lu SM, Li XL, Liu L, Li Z, Liu H and Xu P. Autophagy induction contributes to the resistance to methotrexate treatment in rheumatoid arthritis fibroblast-like synovial cells through high mobility group box chromosomal protein 1. *Arthritis Res Ther* 2015; 17: 374.
- [24] Pan XL, Zhou L, Wang D, Han YL, Wang JY, Xu PD, Zhang HX and Zhou L. Electroacupuncture at “Zusanli” (ST36) promotes gastrointestinal motility possibly by suppressing excessive autophagy via AMPK/ULK1 signaling in rats with functional dyspepsia. *Zhen Ci Yan Jiu* 2019; 44: 486-491.
- [25] Wang MM, Zhang M, Feng YS, Xing Y, Tan ZX, Li WB, Dong F and Zhang F. Electroacupuncture inhibits neuronal autophagy and apoptosis via the PI3K/AKT pathway following ischemic stroke. *Front Cell Neurosci* 2020; 14: 134.